Multiferroic materials and heterostructures / Matériaux et hétérostructures multiferroïques

Novel magneto-electric multiferroics from first-principles calculations

CrossMark

Nouveaux matériaux multiferroïques à partir de calculs de premiers principes

Julien Varignon, Nicholas C. Bristowe, Éric Bousquet, Philippe Ghosez

Theoretical Materials Physics, Université de Liège (B5), B-4000 Liège, Belgique

A B S T R A C T

Interest in first-principles calculations within the multiferroic community has been rapidly on the rise over the last decade. Initially considered as a powerful support to explain experimentally observed behaviours, the trend has evolved and, nowadays, density functional theory calculations have become also an essential predicting tool for identifying original rules to achieve multiferroism and design new magneto-electric compounds. This chapter aims at highlighting the key advances in the field of multiferroics, to which first-principles methods have contributed significantly. The essential theoretical developments that made this research possible are also briefly presented.

© 2015 Académie des sciences. Published by Elsevier Masson SAS. All rights reserved.

R É S U M É

L'intérêt pour les calculs *ab initio* dans la communauté des multiferroïques n'a cessé de croître au cours de la dernière décennie. Ces calculs étaient initialement considérés comme un support efficace pour expliquer les comportements observés expérimentalement, mais la tendance a évolué et, actuellement, les calculs réalisés dans le cadre de la théorie de la fonctionnelle de la densité apparaissent aussi comme un outil prédictif incontournable permettant d'identifier de nouvelles voies pour parvenir au multiferroïsme et créer de nouveaux matériaux magnéto-électriques. Ce chapitre vise à présenter quelques avancées clefs dans le domaine des multiferroïques, auxquelles les méthodes *ab initio* ont conbribué de manière significative. Les développements théoriques essentiels ayant permis ces avancées sont aussi brièvement discutés.

© 2015 Académie des sciences. Published by Elsevier Masson SAS. All rights reserved.

1. Introduction

Discovered at the end of the 19th century, the magneto-electric effect in which the magnetization can be tuned by an electric field and the polarization by a magnetic field has seen significant developments during the 1960–1970s, but remained at that time essentially an academic curiosity. A significant renewal of interest for magneto-electrics has only appeared recently, during the early 2000s [1,2], boosted by their potential for various technological applications [3–6]. The field of magneto-electrics is also intimately linked to that of multiferroics, although not limited to them. It is indeed expected that the amplitude of the linear magneto-electric (ME) effect, α, is bound by the electric (χ^e) and magnetic (χ^m) susceptibilities through the expression $\alpha^2 < \chi^e \cdot \chi^m$ [1]. According to this, the magneto-electric effect can *a priori* be very large in ferroelectrics and/or ferromagnetics and therefore the so-called multiferroic compounds combining these properties have received focussed attention. It is not guaranteed however that these will have the largest magneto-electric coupling.

A quite similar renewal of interest had appeared for ferroelectric compounds a decade before, in the early 1990s. At that time, prototypical ferroelectrics such as $BaTiO_3$ and $PbTiO_3$ had become accessible to density functional theory (DFT) calculations [7]. Initially restricted to explain old observations, the microscopic understanding acquired from first-principles calculations rapidly enabled practical guidance for experimentalists. Theoretical studies played a key role in clarifying the microscopic origin of ferroelectric and piezoelectric properties [7,8] and later ferroelectric finite-size effects [9–11]. In the 2000s, the interest for ferroelectrics then naturally extended to magneto-electric multiferroics.

Over the last decade, first-principles calculations were particularly helpful in the field of multiferroics. On the one hand, they provided microscopic understanding of several experimental observations. They contributed significantly to the understanding of prototypical systems such as $BiFeO_3$ [12], $YMnO_3$ [13,14] or $TbMnO_3$ [15]. On the other hand, first-principles calculations also appear to be a powerful design tool for making theoretical predictions, eventually confirmed experimentally. It is on this second aspect that the present chapter is focussed.

Although not limited to them, many concrete advances to date in the field of multiferroics naturally involved ABO_3 perovskites and related compounds. Thanks to the wide variety of properties they can exhibit within the same simple structure and the possibility to combine them in various nanostructures, these compounds are providing a fantastic playground for both theorists and experimentalists [16]. It was nevertheless initially thought that ferroelectricity and magnetism are mutually exclusive in this class of compounds: the apparent scarcity of ABO_3 multiferroics was explained by the fact that their ferroelectric property is related to O–$2p$–B–$3d$ hybridization and typically requires d^0 occupancy while magnetism requires partial d-state filling [17]. The popular room-temperature multiferroic $BiFeO_3$ (for a more complete discussion, see Y. Yang et al., this issue) circumvents these contradictory B-cation 3d-filling requirements [17] with ferroelectricity and magnetism originating from different A and B cations, respectively. This has motivated the search for related compounds such as Bi_2CrFeO_6, which was predicted to be multiferroic with a large polarization from first principles [18], and later demonstrated experimentally on thin films [19,20]. We will see here that d^0-ness is in fact not always mandatory and that various strategies can be developed to allow ferroelectricity and magnetism to coexist in ABO_3 compounds.

In this paper, we will first briefly describe in Section 2 the essential theoretical advances that were required to make density functional theory calculations predictive and have fuelled theoretical discoveries in the field of multiferroics. Without being exhaustive, we will then present in the next Sections selected strategies that have been proposed to achieve multiferroism and in which theory has played a central role. Although they were at first glance quite distinct, we will see that many of these approaches finally rely on a common concept: how to make a paraelectric magnet ferroelectric. This can be achieved either by strain engineering (Section 3), lattice mode engineering (Section 4) or electronic spin, orbital or charge engineering (Section 5). In all cases a more or less direct magneto-electric coupling is realized. We will briefly address the case of magnetic/ferroelectric interfaces in Section 6, before concluding in Section 7.

We note that the prototypical $BiFeO_3$ system has been extensively studied in the multiferroic community. Due to the volume of work on this material, we will only present a selection of key results coming from first principles and we will refer the reader to the dedicated chapter within this issue for a more complete discussion on this compound.

2. First-principles density functional theory methods

Density functional theory (DFT) was proposed during the mid-sixties. Grounded on the Hohenberg and Kohn theorem [21] and the Kohn and Sham ansatz [22], it was initially a purely theoretical concept that remained dormant for almost 20 years, until the advent of efficient computers enabled its transformation into a very powerful computational method. Since the 1980s, DFT has seen an explosive growth, driven both by the ongoing increase of computer power and various concomitant theoretical and algorithm developments (see for instance the textbook of R.M. Martin for a comprehensive description of DFT [23]). Although *a priori* an exact theory, the practical implementation of DFT relies on approximations giving rise to well-known limitations (see Section 2.3). Nevertheless, the method has proven to be an excellent compromise between accuracy and efficiency. Nowadays, it has become an essential approach in materials research. Aside from the Nobel Prize in chemistry attributed to W. Kohn in 1998 for this specific contribution, it is worth noticing that among the 10 most-cited papers published in the journal *Physical Review*, six are directly related to density functional theory.

First-principles DFT calculations have certainly contributed to the revival of interest for ferroelectrics in the early nineties. The theoretical study of ferroelectrics took advantage of density functional perturbation theory [24,25] to access systematically by linear response various dynamical and piezoelectric properties [26,27] and, reciprocally, contributed to its further

development [28]. It also boosted the discovery of the "modern theory of polarization" by King–Smith and Vanderbilt [29,30] and Resta [31,32]. This fundamental breakthrough allows us to clarify the fundamental role of polarization in periodic DFT [33] and further gave rise to numerous advances, such as the development of finite electric and displacement field techniques [34–36].

Addressing the physics of magneto-electric multiferroics required to face additional new challenges. On the one hand the modelling of magnetic systems is intrinsically much more demanding computationally and methods had also to be developed to access the magneto-electric coefficients. On the other hand, magneto-electric multiferroics are typically strongly-correlated systems for which the usual local density approximation (LDA) or generalized gradient approximation (GGA) to DFT are not appropriate, so that alternative more advanced methods had to be envisaged.

2.1. Magnetic systems

In magnetic compounds, both the spin and the orbital motion of the electrons contribute to the total magnetization. While the spin contribution to the magnetization of periodic solid has been accessible from DFT methods for many years, the way to compute the orbital one has only been formulated recently.

Kohn–Sham DFT can be at first trivially extended to spin-polarized systems by simply treating separately the density of up and down spins [23]. This constitutes a *collinear-spin* level of approximation in which the magnetic moment appears as a scalar quantity. Although widely used, this is not however the most general formulation, since the spin axis can vary in space. Extension of DFT to the *non-collinear spin* level was first formulated by von Barth and Hedin [37]. Here the density is no longer a scalar but a 2×2 matrix $\bar{\bar{n}}(\vec{r})$ depending on the scalar density $\rho(\vec{r})$ and the magnetic density $\vec{m}(\vec{r})$:

$$\bar{\bar{n}}(\vec{r}) = \frac{1}{2}\left(\rho(\vec{r}) \cdot \bar{\mathrm{I}} + \sum_{i=x,y,z} m_i(\vec{r}) \cdot \bar{\bar{\sigma}}_i \right) \tag{1}$$

$$\bar{\bar{n}}(\vec{r}) \quad \Rightarrow \quad \frac{1}{2}\begin{pmatrix} \rho(\vec{r}) + m_z(\vec{r}) & m_x(\vec{r}) - \mathrm{i}\,m_y(\vec{r}) \\ m_x(\vec{r}) + \mathrm{i}\,m_y(\vec{r}) & \rho(\vec{r}) - m_z(\vec{r}) \end{pmatrix} \tag{2}$$

where $\bar{\bar{\sigma}}$ are the Pauli matrices. The spin-density matrix $\bar{\bar{n}}(\vec{r})$ now allows the magnetization to relax in direction and magnitude, providing access to non-collinear magnetic structures. At this level, the coupling between the spins and the lattice has to be explicitly included through the spin–orbit interaction.

Most investigations to date make use of the collinear spin approximation. Although the formalism is well known, non-collinear spin calculations on concrete systems of interest remain very challenging since the energy scale involved is typically extremely small. Calculations require a high degree of convergence and the search for the ground-state spin configuration is complicated by the existence of numerous local minima. Moreover, as further discussed later (see Section 2.3), the final result is often sensitive to the chosen approximations and hence must always be considered with care.

As for the electric polarization, computation of the orbital magnetization in periodic systems remained elusive for many years. The problem has only been solved recently [38,39], providing an expression that can be easily implemented in DFT codes [40]. This can be seen as a Berry phase analogue of the theory of polarization. We refer the reader to Ref. [41,42] for a more complete discussion of the so-called modern theory of magnetization.

2.2. Computing the magnetoelectric coefficients

The magneto-electric tensor α is a mixed second derivative of the energy ($\mathcal{F}$) that describes the change of magnetization (M) produced, at linear order, by an electric field (E) or, equivalently, of polarization (P) produced by a magnetic field (H):

$$\alpha_{ij} = \frac{-1}{\Omega_0} \frac{\partial^2 \mathcal{F}}{\partial E_i \partial H_j} = \frac{\partial P_i}{\partial H_j} = \frac{\partial M_j}{\partial E_i} \tag{3}$$

where Ω_0 is the unit-cell volume. Considering electronic, ionic and strain degrees of freedom as independent parameters (Born–Oppenheimer approximation), α can be conveniently decomposed into three terms:

$$\alpha = \alpha^{\mathrm{el}} + \alpha^{\mathrm{ion}} + \alpha^{\mathrm{strain}} \tag{4}$$

where α^{el} is the purely electronic response (at fixed geometry), α^{ion} the additional contribution coming from the ionic relaxation and α^{strain} the additional contribution coming from the strain relaxation. Keeping in mind that the magnetization can have a spin (S) and orbital (O) origin, α can be viewed as consisting of six individual contributions (see Table 1). Although a key quantity in the study of magneto-electrics, it is worth noticing that the methods providing access to these different terms have only been made accessible recently.

Pioneering computations of the linear magneto-electric coefficients have been performed by Iñiguez et al. Assuming a dominant α_S^{ion} contribution, Iñiguez [44] proposed a scheme to access in a linear response framework the change of spin magnetization resulting from the ionic relaxation produced by an electric field, in a similar spirit as to what is usually done to access the ionic contribution to the dielectric constant [26]. The method was then naturally extended to the strain contribution by Wojdel and Iñiguez [45]. In their derivations, the last two terms of Eq. (4) take the form:

Table 1

Individual contributions to the linear magnetoelectric coupling tensor α. The year it was first computed and the relevant reference are provided in brackets.

	Electronic	Ionic	Strain
Spin	α_S^{el} (2011 [43])	α_S^{ion} (2008 [44])	α_S^{strain} (2009 [45])
Orbital	α_O^{el} (2012 [46])	α_O^{ion} (2012 [46,47])	α_O^{strain} (–)

$$\alpha_{S,ij} = \alpha_{S,ij}^{\text{el}} + \frac{1}{\Omega_0} \sum_{n=1}^{N_{IR}} \frac{p_{ni}^d p_{nj}^m}{K_n} + \sum_{m,n=1}^{6} e_{im} (C^{-1})_{mn} h_{jn} \tag{5}$$

The ionic contribution (second term) involves a sum over the IR active modes; it is directly proportional to the mode di-electric polarity ($p_{ni}^d = \sum_{\text{at}} Z_{\text{at},i}^* u_{ni}$, where Z_{at}^* is the Born effective charge tensor and u_n the phonon eigenvector) and the magnetic equivalent ($p_{ni}^m = \sum_{\text{at}} Z_{\text{at},i}^m u_{ni}$, where Z_{at}^m is the magnetic effective charge tensor [48]) and is inversely proportional to the force constant eigenvalues (K_n). The strain contribution (third term) involves the piezoelectric (e_{im}) and piezomag-netic (h_{jn}) constants and the inverse of the elastic constants matrix (($C^{-1})_{mn}$). Except for p_{nj}^m and h_{jn}, most of the quantities appearing in Eq. (5) were already routinely accessible by linear response or finite difference techniques [27]. In their work, p_{nj}^m and h_{jn} were determined from finite differences. Eq. (5) provides insight into the microscopic origin of α_S^{ion} and α_S^{strain}, suggesting a route to design a large contribution: as proposed in Ref. [49], engineering structural "softness" (vanishingly small eigenvalues of C or K) will produce a diverging behavior.

As an alternative to the previous linear-response approach, Bousquet et al. [43] proposed to access the magneto-electric coefficients from calculations of the change of macroscopic polarization in a finite magnetic field. In their work, the authors proposed to include the effect of the magnetic field through adding a Zeeman term $\overline{\overline{\Delta V}}_{\text{Zeeman}}$ (applied on spins only) to the external potential $\hat{V}_{\text{ext}}$ with the following expression in the 2×2 representation for non-collinear magnetism:

$$\overline{\overline{\Delta V}}_{\text{Zeeman}} = \frac{-g}{2} \mu_B \mu_0 \begin{pmatrix} H_z & H_x + i H_y \\ H_x - i H_y & -H_z \end{pmatrix} \tag{6}$$

where $\vec{H}$ is the applied magnetic field. The magneto-electric coefficients are then deduced from calculations at different amplitudes of the field by finite difference: $\alpha_{S,ij} = \Delta P_i / \Delta H_j$. On the one hand, calculations in finite H field at fixed ionic positions and strains have given access for the first time to α_S^{el}. On the other hand, calculations including structural relaxation provide alternative access to α_S^{ion} and α_S^{strain}. Although in multiferroics α_S^{ion} is expected to dominate especially around the ferroelectric phase transition, Bousquet et al. have shown that in the magneto-electric Cr_2O_3, α_S^{el} is comparable in magnitude to α_S^{ion} and therefore by no means negligible. It is worth noticing also that such a finite field approach is not restricted to the determination of α but extends also to higher-order responses.

The calculation of the orbital magnetic response came slightly later, with the emergence of the modern theory of mag-netization [50–52]. Using this technique, Malashevich et al. [46] computed α_O^{el} and α_O^{ion} for Cr_2O_3 from the change of M in an E field and they indeed confirmed that the orbital contribution is much smaller than the spin one. At the same time, Scaramucci et al. [47] computed α_O^{ion} in $LiFePO_4$. They used the approximation of integrating the orbital moment with spheres centred on each atom instead of the exact modern theory treatment and studied α_O^{ion} using a method similar to that of Iñiguez [44]. Interestingly, these results show that α_O^{ion} in $LiFePO_4$ is as large as α_S^{ion} and is even as large as the full ME response of Cr_2O_3.

Alternative methods have been designed to overcome the fact that only the spin contribution at 0 K is taken into account in the calculation of the ME response within DFT. As the temperature increases, spin fluctuations arise and can induce an additional contribution to α^{spin}. This is the so-called exchange–striction mechanism. Mostovoy et al. developed a method to take into account this temperature effect by combining Monte-Carlo simulations on a Heisenberg-type Hamiltonian in which the exchange parameters were calculated from DFT calculations [53]. They applied their method on Cr_2O_3 and showed that the exchange–striction mechanism can induce a non-zero and large ME response along a direction that would be zero otherwise. The spin fluctuations break the inversion center and induce a polarization in the crystal. They also showed that the spin–orbit origin of the ME response is one order of magnitude smaller than the exchange–striction contribution when it reaches its maximum at a given temperature.

The linear and non-linear magneto-electric coefficients at finite temperature and the origin of the spin spiral of $BiFeO_3$ have also been calculated in the framework of an effective Hamiltonian [54,55].

2.3. Beyond LDA and GGA

By default, DFT calculations are performed within the so-called Local Density Approximation (LDA) or Generalized Gra-dient Approximations (GGA). Although these have proven to be highly predictive for many classes of compounds such as band insulators and simple metals, they fail to describe systems with strong electronic correlations (see Ref. [23]).

Since multiferroics involve correlated systems, more advanced functionals are required to capture the basic physics. The most simple and popular approach is the LDA + U method, which involves two empirical parameters U and J, accounting for the on-site Coulomb interactions and the intra-site spin exchange respectively [56]. Both are captured in an effective way through a Hubbard-like model. Two different implementations of LDA + U are commonly used: one adopting two independent parameters [57] and the other using only one effective parameter $\Delta U_{\text{eff}} = U - J$ [58]. In either case, U and J (or ΔU_{eff}) are adjustable parameters and one must fit their value in order to reproduce experimental trends. Alternatively, a self-consistent method to calculate the parameters exists [59]; however it does not always appear to be fully predictive and the parameters sometimes have to be rescaled [60]. In practice, the basic properties of the material are extremely sensitive to the values of U and J. While at the spin collinear level, J is commonly neglected, this parameter becomes important and meaningful when going to non-collinear spin calculations as it acts on the off diagonal terms of Eq. (2), in other words on the spin canting of the system [61].

In order to overcome the adjustable parameters of LDA + U, hybrid functionals are a valuable alternative method that has become widely used nowadays [62–66]. These functionals take their name from the fact that they consist of a combination of LDA and GGA functionals plus a part of exact exchange to reproduce exchange and correlation effects more accurately. The most famous hybrid functionals are the B3LYP [67] and HSE [68]. A B1WC functional has also been optimized for ABO_3 ferroelectrics [69] and proved powerful for multiferroics as well [62,64,65]. Unfortunately, these hybrid functionals are not widely implemented in DFT codes, and additionally are more computationally expensive. Consequently, some groups are then using them as a benchmark to extract the adjustable parameters for a more computationally tractable LDA + U calculation [66].

While LDA + U and hybrid functionals are the most commonly used approach within the field of multiferroics, several alternative methods exist. In order to remedy failures in DFT arising from the spurious self-interaction term (interaction of an electron with the potential generated by itself), Filippetti and Spaldin proposed a method to better approximate the correction to this term within pure LDA calculations, involving minimal computational costs (pseudo-Self Interaction Correction method) [70]. Dynamical Mean Field Theory (DMFT) is an alternative method to describe correlation effects by going beyond the static mean field theory used in DFT [71,72]. Alternatively, a quantum chemistry method has been developed to accurately evaluate magnetic couplings in strongly correlated systems [73] and has been used to study the evolution of the magnetic exchange integrals with an external electric field [74]. The most accurate but expensive parameter-free theoretical method including many body effects is the GW method, which has been used as a benchmark for DFT calculations on $BiFeO_3$ [63].

We conclude the section by emphasizing that DFT calculations are restricted to 0 kelvin in practice. In the field of ferroelectrics, this limitation has been elegantly overcome through the developments of a so-called effective Hamiltonian method as pioneered by Zhong, Rabe and Vanderbilt [75,76]. This method has been generalized by Bellaiche and co-workers for the case of multiferroics [60]. So far it has been applied to $BiFeO_3$, yielding many key advances [55,77–80].

3. Strain engineering

During the early 2000s, much effort was devoted to the understanding of the role of electrical and mechanical boundary conditions on the ferroelectric properties of ABO_3 perovskite thin films [10,11]. In 2004, it was shown, for instance, that $SrTiO_3$, which is paraelectric at the bulk level, can be made ferroelectric in thin film form and develop a spontaneous polarization at room temperature under moderate epitaxial tensile strain [81]. The idea naturally emerged to apply a similar strategy to turn paraelectric magnets into ferroelectrics and make them *de facto* multiferroics.

3.1. Inducing ferroelectricity by strain in magnetic systems

Strain engineering of ferroelectricity is quite a universal approach, based on polarization (P)–strain (η) coupling. In simple cubic perovskites, this P–η coupling contributes to the Landau free energy $\mathcal{F}$ through a term of the form (at the lowest order):

$$\mathcal{F}(P, \eta) \approx g\eta P^2 \tag{7}$$

In non-ferroelectric compounds, the curvature of the energy with respect to the polarization is positive at the origin (red curve in Fig. 1). From Eq. (7), it appears that one effect of the strain is to renormalize this energy curvature. When producing a sufficiently large negative contribution, the polarization–strain coupling can hence destabilize the system and make it a proper ferroelectric (blue curve in Fig. 1). We notice that turning the system into a ferroelectric is *a priori* possible, whatever the sign of the electro-strictive coefficients g, through an appropriate choice of the strain (compressive or tensile). In practice, the feasibility of the approach relies however on the amplitude of the requested strain. So, starting from compounds on the verge of ferroelectricity is clearly an asset.

As a concrete illustration of strain-induced ferroelectricity in magnetic systems, let us consider $CaMnO_3$, a well-known G-type anti-ferromagnetic (AFM-G) insulator. At the bulk level, $CaMnO_3$ exhibits a paraelectric *Pnma* orthorhombic structural ground state, consisting of a slight distortion of the ideal perovskite structure produced by antiferrodistortive (AFD) oxygen motions. Using first-principles calculations, Bhattacharjee et al. [83] have shown that, in its cubic phase, $CaMnO_3$ does in
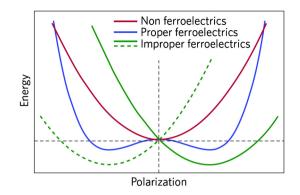
Fig. 1. (Color online.) Energy potential as a function of the polarization. Figure taken from Ref. [82].

fact combine weak ferroelectric (FE) and strong AFD instabilities. Although the former is suppressed by the appearance of the oxygen motions in the *Pnma* phase, they predicted that orthorhombic CaMnO$_3$ can be made ferroelectric under moderate epitaxial tensile strain, which was subsequently confirmed experimentally [84]. Additionally, they also pointed out that the FE distortion in CaMnO$_3$ is dominated by the Mn motion, demonstrating that, in contrast to the previously discussed d^0 rule [17], the same cation can be responsible for the magnetic and ferroelectric properties.

Inducing ferroelectricity by strain in a magnetic compound such as CaMnO$_3$ makes it multiferroic, but does not necessarily guarantee strong magneto-electric coupling. Bousquet and Spaldin [85] nevertheless highlighted in 2011 that the appearance of a spontaneous polarization in *Pnma* perovskites can also give rise to a linear magneto-electric effect. In the *Pnma* phase, the symmetry allows for a small canting of the otherwise anti-ferromagnetically ordered spins, yielding weak ferromagnetism [86]. A center of inversion is preserved however, in which case weak ferromagnetism is incompatible with a linear magneto-electric effect [87]. Inducing ferroelectricity by strain breaks the inversion symmetry and additionally offers the possibility of achieving a linear magneto-electric coupling. In the resulting ferroelectric *Pmc*2$_1$ phase adopted by CaMnO$_3$ under moderate epitaxial tensile strain, Bousquet and Spaldin predicted a linear magneto-electric coefficient much larger than that of more conventional magneto-electrics like Cr$_2$O$_3$. Their analysis, based on symmetry arguments, is totally general. Since the *Pnma* structure is the most common ground state in ABX$_3$ compounds, this finding generates a tremendous number of possibilities for creating new magneto-electric materials under epitaxial strain.

Although not related to strain engineering, we notice here that the interplay between ferroelectric distortion and weak ferromagnetism had also been discussed independently by Fennie [88]. The author proposed design rules for identifying compounds in which ferroelectric distortions can induce weak ferromagnetism. In such cases, the weak magnetic moment is directly proportional to P: switching one will automatically switch the other, therefore opening the door to electric switching of the magnetization. Using first-principles calculations, he proposed *R*3*c* FeTiO$_3$ and related compounds as a promising realization of these ideas. It was further confirmed experimentally that the *R*3*c* phase of FeTiO$_3$ is indeed ferroelectric and a weak ferromagnet [89].

Strain engineering can give rise to other unexpected phases in bulk perovskites such as the supertetragonal T phase (under compression) [90,91] or the *Pmc*2$_1$ phase (under tension) of highly-strained BiFeO$_3$ [92,93] or in superlattices such as the ferromagnetic–ferroelectric *Pc* phase of SrTiO$_3$/SrCoO$_3$ [94]. Besides ABO$_3$ perovskites, simple magnetic AO binary oxides surprisingly also appear as promising candidates to multiferroism through epitaxial strain. Bousquet et al. [95] proposed that EuO can be made ferroelectric under experimentally achievable epitaxial strains. Combined with the ferromagnetic character of EuO, this would open interesting new perspectives if experimentally verified.

Moreover, strain engineering is not restricted to the possibility of inducing ferroelectricity in paraelectric magnets. It can also be used to monitor the properties of regular magnetoelectrics. From their calculations, Wojdel and Iñiguez have shown the possibility to achieve a large enhancement of the linear magnetoelectric coupling by inducing "structural softness" (see Section 2.2) through epitaxial strain in BiFeO$_3$ films [49]. In that study, they exploit the fact that, under compressive epitaxial strain, BiFeO$_3$ exhibits a structural phase transition from a ferroelectric rhombohedral to a ferroelectric supertetragonal T phase. Close to the critical strain, there is a region where the compound becomes structurally soft and displays large responses. Strain can further be used to tune the magnetic properties of the T phase of BiFeO$_3$ [96]. Another example where strain is used to tune the competition between alternative ordered phases is provided in the next section.

3.2. Exploiting large spin–lattice coupling

In magnetic systems, the optical modes at the zone-center, consisting of relative motions of distinct sublattices, are able to affect spin–spin couplings. The frequency ω of the zone-center optical modes are therefore expected to be particularly dependent on the spin arrangement. This is the so-called "spin–lattice" coupling that can be approximated as [97–99]:
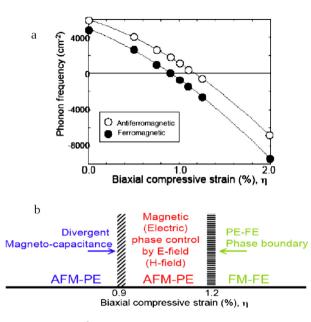
$$\omega \approx \omega_{\mathrm{PM}} + \gamma \langle \mathbf{S}_i \cdot \mathbf{S}_j \rangle \tag{8}$$

Fig. 2. (Color online.) (a) Evolution of the polar frequency ω^2 as a function of the compressive strain η within a ferromagnetic (filled circles) and antiferromagnetic (unfilled circles) ordering. (b) Phase diagram of EuTiO$_3$ as a function of the compressive strain η.
Figures reprinted with permissions from C.J. Fennie, K.M. Rabe, Phys. Rev. Lett. 97 (2006) 267602 (Ref. [99]).
© 2014 by the American Physical Society.

where ω_{PM} is the frequency in the paramagnetic state, γ is the spin–lattice coupling constant and $\langle \mathbf{S}_i \cdot \mathbf{S}_j \rangle$ the nearest-neighbour spin–spin correlation function. This coupling in fact gives rise to a non-linear magneto-electric effect, whatever the symmetry of the magnetic system. In displacive ferroelectrics, the ferroelectric phase transition is driven by the softening of a polar zone-center mode that condenses at the phase transition, producing a finite spontaneous polarization [100]. When γ is substantial, the spin–lattice coupling will produce additional tuning of the soft-mode. In a simple Landau expansion of the free energy, the essential physics of this tuning behavior can be included through a bi-quadratic term [101]:

$$\mathcal{F}(P, M) \approx -\gamma' M^2 P^2 \qquad \mathcal{F}(L, M) \approx +\gamma' L^2 P^2 \tag{9}$$

where M and L are the ferromagnetic and antiferromagnetic order parameters. As for the strain in Eq. (7), we see that the magnetic order is able to renormalize the curvature of the energy versus the polarization curve. By tuning the system through an external parameter such as strain, the critical value of the parameter that can make the system ferroelectric will hence depend on the magnetic configuration.

Using first-principles calculations, Fennie and Rabe [99] proposed to exploit this effect in EuTiO$_3$, an antiferromagnetic insulating perovskite that, in bulk, remains cubic and paraelectric at all temperatures. This system exhibits a large and positive spin–lattice coupling that further stabilizes the paraelectric state in the AFM configuration (positive term in Eq. (9)) over a hypothetical FM state (negative term in Eq. (9)). Exploiting strain to induce ferroelectricity in EuTiO$_3$ (compressive or tensile strain can be used due to the opposite g coefficient associated with in-plane and out-of-plane P in Eq. (7)), the amplitude of the critical strain needed to make the system ferroelectric will be smaller for the FM state (η_c^{FM}) than for the AFM one (η_c^{AFM}) (Fig. 2a). They demonstrated that in the intermediate strain region $|\eta_c^{FM}| < |\eta| < |\eta_c^{AFM}|$, the system offers easy magnetic control of the polarization (and *vice-versa*): in this region, the system is still an AFM paraelectric and aligning the spins in a magnetic field (inducing a polarization with an electric field) will induce a substantial polarization (magnetization) by switching the system to the alternative FM ferroelectric state (Fig. 2b). Going further, they highlighted that under sufficiently large epitaxial strain the system will even adopt a FM ferroelectric ground state. This was further confirmed experimentally [101], offering a practical way to create ferroelectric ferromagnets.

Although this constitutes a nice proof of concept, the practical use of EuTiO$_3$ will be limited by its extremely low Néel temperature ($T_N \simeq 5.5$ K). In the search of alternative systems realizing the same ideas, it might be interesting to look for compounds having magnetic ordering temperatures as high as possible. However, this is limited by the fact that the difference of energy between FM and AFM states cannot be too different from the energy gain produced by the ferroelectric distortion. SrMnO$_3$ exhibiting moderate Néel temperature ($T_N \simeq 233$–260 K [102]) and large spin–phonon coupling was identified by Lee and Rabe [103] as a good candidate. They showed that increasing epitaxial strains (both tensile and compressive) brings the system into a ferroelectric–ferromagnetic ground state through a complex sequence of consecutive phase transitions.

Again such a general strategy might be applied to other classes of compounds. For instance, MnF$_2$ [104] was shown to exhibit a low-frequency polar mode, slightly softening with temperature and exhibiting a sizable spin–lattice coupling.

4. Lattice-mode engineering

Beyond strain engineering, alternative strategies can be envisaged to create new multiferroics. In this section we will discuss how the coupling of polar modes with non-polar instabilities can be exploited to produce a polar ground state in magnetic compounds.

4.1. Improper and hybrid improper ferroelectrics

$YMnO_3$ is a well-known multiferroic, which due to its small tolerance factor, prefers a hexagonal packing to the cubic perovskite form. At the structural level, it exhibits a structural phase transition from a paraelectric $P6_3/mmc$ phase to a ferroelectric $P6_3cm$ ground state, involving unit cell tripling. As evidenced at the first-principles level by Fennie and Rabe [13], there is no ferroelectric instability at the zone-center in the $P6_3/mmc$ phase. The phase transition is produced by the condensation of an unstable zone-boundary K_3 mode that, in turn, produces the appearance of an additional polar distortion through a coupling term in the energy of the form:

$$\mathcal{F} \approx \lambda \mathcal{Q}_{K_3}^3 P \tag{10}$$

where $\mathcal{Q}_{K_3}$ is the amplitude of the K_3 mode.[1] Such compounds in which the polarization appears as a slave of another non-polar primary order parameter with which it couples through a term linear in P is called an improper ferroelectric [106]. In contrast to the strain coupling in Eq. (7) that renormalizes the curvature at the origin of the energy versus the polarization well, the *improper* coupling in Eq. (10) induces ferroelectricity by shifting this well, as illustrated by the green curves in Fig. 1. Improper ferroelectrics consequently behave differently than proper ferroelectrics. Importantly, switching the polarization will necessarily require switching the primary non-polar order parameter (dashed green line in Fig. 1). Also, improper ferroelectrics exhibit distinct dielectric properties [106] and are less sensitive to depolarizing field issues [107,108].

A similar improper behavior was recently predicted theoretically by Varignon and Ghosez [64] in 2H-$BaMnO_3$, in spite of a completely different atomic arrangement, cation sizes, and Mn valence state, compared to $YMnO_3$. In simple cubic perovskites, zone-boundary antiferrodistortive (AFD) instabilities associated with the rotation of oxygen octahedra are very frequent. However, by symmetry, these modes cannot couple with polarization through a term linear in P to produce improper ferroelectricity.[2] The situation is however distinct in layered perovskites [110].

In 2008, Bousquet et al. [111] reported a new type of improper ferroelectricity in $PbTiO_3$/$SrTiO_3$ short-period superlattices epitaxially grown on $SrTiO_3$. From first-principles calculations, they revealed that the ground state of $PbTiO_3$/$SrTiO_3$ 1/1 superlattices exhibits a complex ground state combining two independent AFD motions and one ferroelectric distortion sketched in Fig. 3 and hereafter referred to as ϕ_1, ϕ_2 and P, respectively. They highlighted that, by symmetry, these three modes couple through a trilinear energy term of the form:

$$\mathcal{F} \approx \lambda \phi_1 \phi_2 P \tag{11}$$

They argued that in systems where ϕ_1 and ϕ_2 instabilities dominate, this term can give rise to ferroelectricity in a way similar to Eq. (10). In this case, however, two independent non-polar modes of different symmetry are involved and the term "hybrid improper ferroelectricity" has been coined by Benedek and Fennie [112] to label such systems.

Since then, the trilinear coupling of lattice modes in perovskite layered structures has generated increasing interest. Further investigations have been since performed on $PbTiO_3$/$SrTiO_3$ superlattices, clarifying the role of the strain on the relevant AFD motions and the polarization [113]. Alternative trilinear couplings have been obtained [112,114–116]. Guiding rules to identify alternative hybrid improper ferroelectrics have been proposed [115] and the emergence of ferroelectricity in rotation-driven ferroelectrics was discussed [117]. Finally, novel improper couplings have been revealed in alternative A-cation ordered structures such as the [111]-rocksalt arrangement [118].

4.2. Toward electric control of the magnetization

As in regular improper ferroelectrics, the switching of the polarization in hybrid improper ferroelectrics will necessarily be associated with the switching of another non-polar mode (either ϕ_1 or ϕ_2). It had been suggested by Bousquet et al. [111] that the intimate link between polar and AFD motions produced by the trilinear term could be exploited to tune the magnetoelectric response.

Benedek and Fennie [112] proposed to realize this in $Ca_3Mn_2O_7$, a naturally occurring Rudlesden–Popper layered compound. Using first-principles calculations, they showed that in this system two AFD motions not only combine together

---

[1] As initially performed in the seminal work of Fennie and Rabe [13], we restrict here the free energy expansion to a bidimensional subspace restricted to the zone-center and K_3 modes that are condensing. A more complete expression including the full invariants in the free energy expansion of hexagonal manganites can be found in Ref. [105].

[2] Hybrid improper ferroelectricity can occur in bulk cubic perovskites but involves additional anti-polar modes [93,109].
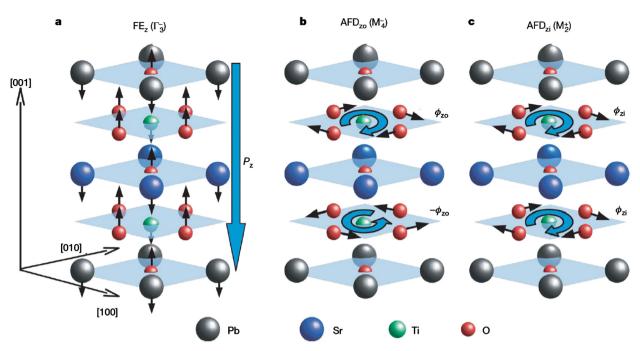
Fig. 3. (Color online.) Schematic view of the polar mode (a) and the two AFD motions (b and c). Picture taken from Ref. [111].

to induce a polar distortion through Eq. (11), but also produce weak ferromagnetism and a linear magneto-electric effect. They proposed that under appropriate strain engineering of the energy landscape, it might be possible to realize electric switching of the magnetization in such systems.

A similar type of hybrid improper ferroelectricity has recently been reported in alternative magnetic systems such as $NaLaMnWO_6$ [114] or $RLaMnNiO_6$ [119] double perovskites, $BiFeO_3/LaFeO_3$ superlattices [120] and even in metal–organic frameworks [116].

Some effort has been devoted recently to rationalize the concept of improper ferroelectrics from finite electric displacement calculations at 0 K [108]. Still at this stage, several important questions remain open regarding these materials. For example, uncertainties remain concerning their finite temperature properties and in particular the phase transition mechanism [110]: for example, are there single or consecutive phase transitions, or an avalanche mechanism [121]? Another central issue also concerns the ferroelectric switching path and associated energy barrier. As highlighted from the first-principles calculations in Ref. [120], the path with the lowest energy barrier seems to be quite complex, but compatible with the reversal of the magnetization. To begin to understand these issues further, finite-temperature molecular dynamics using effective Hamiltonians, along with further experimental efforts, are likely to play a key role in the future.

Trilinear couplings with the polarization are not restricted to AFD motions, but can alternatively include Jahn–Teller motions [116] or anti-polar motions [93,109]. This opens the possibility to realize similar phenomena in bulk perovskites. In the identified $Pmc2_1$ phase of highly strained $BiFeO_3$, a trilinear term, $M_{AP}\Phi P$, involving an anti-polar mode (M_{AP}), one rotation (Φ) and the polarization P was discovered and predicted to allow for an electrical control of magnetization [93].

5. Inducing electronic polarization in magnets through charge, spin and orbital ordering

In the previous sections, we have primarily discussed how strain and lattice mode couplings can induce a ferroelectric polarization and how this can help to design new multiferroics. A different class of multiferroics exists where it is the electronic degrees of freedom (charge, spin or orbital) that instead lower the symmetry of the system and produce ferroelectricity. The resultant electronic polarization is expected to be small but can range from $nC \cdot cm^{-2}$ to several $\mu C \cdot cm^{-2}$. The advantages here include potentially faster polarization switching involving electron rather than ionic dynamics, and substantially larger magnetoelectric coupling since magnetism and ferroelectricity can share the same microscopic origin.

First-principles calculations are ideally suited for the study of subtle microscopic electronic phenomena and elucidating novel electronic multiferroics has been one of the main focuses within the first-principles community over the last few years. Whilst the field of electronic multiferroics is still in its infancy, exciting new results are constantly being obtained and first-principles calculations have often played a key role. Below we very briefly highlight some examples. For further discussions on this topic we refer the reader to the article by P. Barone & S. Picozzi in this issue, and to the recent review of Barone and Yamauchi [122].

5.1. Spin ordering induced ferroelectricity

In some systems, traditionally labelled as type-II multiferroics, the spin order helps to break the inversion symmetry, which can lead to a polar ferroelectric state. A prototypical example of this is the orthorhombic perovskite $TbMnO_3$ where the non-collinear cycloidal-spin structure generates an electric polarization via the spin–orbit interaction. Although the polarization might be thought as purely electronic in nature in such systems, it was clarified by Malashevich and Vanderbilt [123] that, in $TbMnO_3$, the dominant contribution comes from the subsequent lattice relaxation.

In the same spirit, it was discovered that ferroelectric polarization can also be inherent to a collinear E-type antiferromagnetic (AFM-E) order. The AFM-E ordering consists of up–up–down–down spin ordering, through FM nearest neighbour and AFM next nearest neighbour interactions, as observed in several orthorhombic perovskite manganites $RMnO_3$ [124,125] and monoclinic nickelates $RNiO_3$ [126]. First-principles calculations have been a very powerful tool in solving the origin of the polarization in these particular cases. For instance, DFT calculations were able to validate that AFM-E induces ferroelectricity in one of the prototypical compounds $HoMnO_3$ [127,128] and to explain the relatively small polarization measured in $HoMn_2O_5$ and $TbMn_2O_5$, understood as a cancellation of the contribution coming from the atomic displacements and the electronic part due to strong electronic correlations [129,130]. This electronic polarization has been shown to exist without the need of any lattice displacements, or spin–orbit interaction, as observed in YMn_2O_5 [131].

5.2. Charge ordering induced ferroelectricity

Another route to create electronic polarization is achieved by charge ordering through mixing cations with different valence states. This was first proposed by Efremov et al. [132] in the doped manganites ($Pr_{0.4}Ca_{0.6}MnO_3$ for instance [133,134]) and where first principles calculations provided important microscopic understanding [135].

A similar mechanism occurs in the well-known magnetite Fe_3O_4 compound. Magnetite, the first magnetic system ever to be identified, was known for decades to develop ferroelectricity at low temperature [136], but its origin was highly debated. Recent DFT calculations from Picozzi et al. [137] demonstrated the charge ordering between Fe^{2+}/Fe^{3+} to be responsible for the experimentally measured and switchable polarization [138].

A debate is still ongoing for the similar ferrimagnetic magnetoelectric spinel $LuFe_2O_4$. Indeed, it was proposed that the charge ordering between Fe^{2+}/Fe^{3+} on consecutive triangular Fe bilayers was responsible for polarization [139], making $LuFe_2O_4$ the ideal charge-ordered induced multiferroic. Eventually, a recent joint X-ray plus DFT study proposed an antiferroelectric charge-ordered ground state [140]. First-principles calculations also predict related spinels to be good candidates to reach an electronic ferroelectric multiferroic system, such as in vanadium-based spinels ZnV_2O_4 [141] or CdV_2O_4 [142] or Fe-based systems that are predicted to show a large magnetoelectric effect [143].

Following the same spirit, Picozzi et al. [144] proposed the tetragonal tungsten bronze $K_{0.6}FeF_3$ as a prototypical charge-ordered-induced ferroelectricity, and a novel playground for multiferroicity. Based on first-principles calculations, various Fe^{2+}/Fe^{3+} charge ordering patterns were found to produce polarizations with different directions and magnitudes.

5.3. Orbital ordering induced ferroelectricity

The third electronic degree of freedom, orbital ordering, is also proposed as a route to engineer ferroelectricity, however it is commonly linked (induced) to (by) a charge or spin ordering, and remain more elusive. For instance, Ogawa et al. propose on the basis of a joint Second Harmonic Generation and DFT study that the orbital ordering appearing in some shear-strained half-doped manganite thin films is linked to an off-centering of the cations [145]. Orbital ordering has been predicted to produce ferroelectricity at the ultra-thin film limit in $SrCoO_3$ [146]. Through partial substitution of Ti^{4+} ($3d^0$) by magnetic vanadium ($3d^1$) ions in non-magnetic $La_2Ti_2O_7$, Scarrozza et al. demonstrated that a multiferroic behaviour is reached with a sizeable polarization of $4.5\ \mu C \cdot cm^{-2}$ at 12% of doping arising from combined orbital ordering and V–V dimerisation symmetry breaking.

6. Interface magnetoelectricity

Whilst recent progress has been made in bulk single-phase magneto-electrics (including superlattices), special attention was also devoted to multi-component/composite systems, where the search is less constrained, and the magneto-electric effect may be substantially larger. This topic has been the focus of intensive research over the last decade, with two main strategies surfacing. The traditional approach uses the strain coupling at an interface between a piezoelectric material and a piezomagnetic one [147]. The polarization and magnetization coupling is mediated by strain, which can be a longer-range effect penetrating into the bulk of each material. The second strategy is more fundamental: since any interface/surface of a material breaks spacial inversion symmetry, if one of the two components is ferromagnetic, which additionally breaks time reversal, a linear magnetoelectric effect can be expected [148]. This section will provide only a brief overview of the second strategy, which relies on subtle alterations of chemistry, bonding, structure and electronics at the interface, and hence where first-principles calculations have proved invaluable. For more comprehensive reviews, we refer the reader to references [87,149–152].
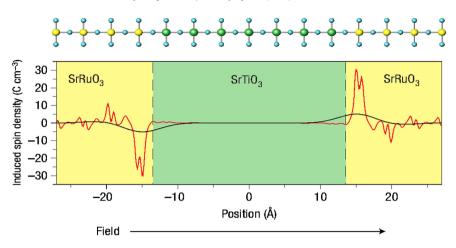
Fig. 4. (Color online.) Electric-field-induced interface magnetization from first-principles calculations of a $SrTiO_3$–$SrRuO_3$ capacitor [159]. Red and black lines are the calculated planar and macroscopically averaged induced magnetizations, respectively. Figure taken from Ref. [159].

Interface systems create two additional theoretical challenges over bulk systems. Firstly, the task of modelling metal–insulator capacitor systems under finite electric field. Secondly the problem of band alignment at metal–insulator interfaces with DFT which famously underestimates band gaps [11]. These two challenges have only been considered in recent years [153–155]. Several DFT codes can now routinely examine capacitor systems under various electrical boundary conditions, and many studies are now closely analysing the effect of band-gap correcting functionals on metal–insulator heterostructures (see for example references [156,157]).

With these recent advances in theoretical methodologies, first-principles calculations are leading the way in the field of magnetoelectric interfaces [158], not only in the fundamental understanding of experimental observations, but interestingly in the prediction of new phenomena. One striking example is the study of Rondinelli et al. [159], where a novel carrier-mediated magnetoelectric effect was demonstrated at the $SrRuO_3$/$SrTiO_3$ interface. The effect was argued to be a universal feature of metallic–ferromagnetic/dielectric interfaces, where spin-polarized carriers within the metal accumulate or deplete in the interface region in an attempt to screen the capacitive/bound charges arising at the interface under an electric field (see Fig. 4). The effect was argued to be magnified when the dielectric is replaced with a ferroelectric, here $BaTiO_3$ (BTO), and if the metal displays a high-spin polarization at the Fermi level, whilst low total magnetization (as in a half-metallic antiferromagnet) [159,160]. First-principles calculations have observed related carrier-mediated magnetoelectric effects, though substantially weaker, at magnetic metallic surfaces, such as $SrRuO_3$ [160], Fe_3O_4 [161], and Fe, Co and Ni [162].

At the $Fe/BaTiO_3$ interface, calculations suggested an induced moment on interface Ti atoms, whose magnitude depends on the $BaTiO_3$ polarization direction [163,164]. Authors ascribed a mechanism based on local atomic distortions at the interface. Depending on the polarization direction, hybridization between Ti 3d and Fe 3d strengthens or weakens, altering the moment on Ti. This explanation has recently been challenged within reference [155], where the authors suggested that the aforementioned problem related to pathological band-offsets within DFT may be playing a role. A more recent DFT + U study correcting for the band gap, ascribed the magnetoelectric coupling as a combination of hybridization and carrier-mediated processes [165]. Similar hybridisation-driven magnetoelectric effects have also been predicted from first-principles calculations for $Fe/PbTiO_3$ [164], $Co_2MnSi/BaTiO_3$ [166], and $Fe_3O_4/BaTiO_3$ [167] interfaces.

First-principles calculations on similar metallic–magnetic/insulator systems have observed a range of additional fascinating phenomena. Namely the electric field has been predicted to tune not only the magnitude of the magnetic moments, but also the magnetic ordering, the magnetic easy axis and the magnetic Néel temperature. Each of these mechanisms is described briefly below.

The carrier mediated effect described above can be viewed as a local change in the doping concentration near the interface. In materials such as the doped manganites (e.g., $La_{1-x}Sr_xMnO_3$), the doping concentration plays a dramatic role on the physical properties of the material, in particular magnetic ordering. First-principles calculations elucidated such an effect at an interface between $La_{1-x}A_xMnO_3$ (A = Ca, Sr, Ba) and BTO [168]. Depending on the direction of the polarization in $BaTiO_3$, the ground-state magnetic phase was found to be either ferromagnetic or A-type AFM locally at the interface [157, 168,169].

In addition to the electric-field-induced changes in the magnitude of the magnetic moment, or the magnetic ordering, first-principles calculations have predicted the possibility of electric-field tuning of the interface/surface magnetic easy axis [162,170–175]. The alteration of the magnetocrystalline anisotropy was argued to arise from field driven changes in the relative occupations of the t_{2g} orbitals for the case of Fe/MgO [174] and several ferromagnetic metallic surfaces [162,171]. For the $Fe/BaTiO_3$ interface the effect was instead thought to arise from Ti 3d–Fe 3d hybridisation modifications [170]. Recently, first-principles calculations have predicted a 180° switch in the magnetization at the $Fe/PbTiO_3$ interface through reversal of the polarization [176]. This was produced by utilizing the magnetic interlayer exchange coupling with a capping FM/nonmagnetic/FM trilayer.

We can also mention the predicted and demonstrated enhancement of the Curie temperature in a ferromagnetic–ferroelectric superlattice [177]. The effect was argued as a modification of the orbital ordering arising on Mn 3d orbitals in $La_{1-x}Sr_xMnO_3/BaTiO_3$ superlattices, which can affect the strength of the FM double-exchange mechanism through enhancing orbital overlap. The role of the polarization of ferroelectric $BaTiO_3$ here was not discussed, only the epitaxial strain mismatch. However, the calculations revealed a large asymmetry on Mn interface moments, which is an indication of spin-polarized-carrier screening of the ferroelectric polarization. Ferroelectric distortions have recently been argued to play a role in the orbital ordering in related $PbTiO_3$–$La_{1-x}Sr_xMnO_3$ superlattices [178] through first-principles calculations.

Finally, it is worth noticing that it is not necessary to combine distinct materials to create interfaces. Ferroic compounds naturally develop domain walls, separating regions with different orientations of the ferroic order. Owing to the symmetry breaking and local mechanical constraints, these natural boundaries can exhibit properties distinct from those of the domains surrounding it. Recently, new exciting phenomena have been reported at domain walls in multiferroics [179–181], opening novel possibilities to achieve magnetoelectricity as for instance in hexagonal manganites and ferrites [182,183].

7. Conclusions

Over the last twenty years, first-principles methods have proven their effectiveness within the field of multiferroics, both for explaining phenomena and designing novel materials. In this chapter, we have summarized the advances in the theoretical methodologies and the key discoveries that the methods have fuelled. Naturally the multiferroic community has focussed on the ABO_3 perovskites, likely due to historical reasons with the push from the ferroelectric section. With the first-principles conception of several design strategies for novel multiferroics, perhaps the future focus should be the targeting of new promising classes of materials other than perovskites. In this respect, the combination of these design strategies, along with the rapid rise of the so-called high-throughput [184–187] first-principles calculations, could pave the way for future multiferroic design.

Acknowledgements

References

[1] M. Fiebig, J. Phys. D, Appl. Phys. 38 (2005) R123.
[2] W. Eerenstein, N. Mathur, J. Scott, Nature 442 (2006) 759.
[3] M. Bibes, A. Barthélémy, Nat. Mater. 7 (2008) 425.
[4] T. Kimura, T. Goto, H. Shintanl, K. Ishizaka, T. Arima, Y. Tokura, Nature 426 (2003) 55.
[5] N. Hur, S. Park, P.A. Sharma, J.S. Ahn, S. Guha, S.W. Cheong, Nature 429 (2004) 392.
[6] T.G.T. Kimura, G. Lawes, A.P. Ramirez, Y. Tokura, Phys. Rev. Lett. 92 (2004) 257201.
[7] R.E. Cohen, Nature 358 (1992) 136.
[8] D. Vanderbilt, Curr. Opin. Solid State Mater. Sci. 2 (1997) 701.
[9] J. Junquera, P. Ghosez, Nature 422 (2003) 506.
[10] M. Dawber, K. Rabe, J. Scott, Rev. Mod. Phys. 77 (2005) 1083.
[11] J. Junquera, P. Ghosez, J. Comput. Theor. Nanosci. 5 (2008) 2071.
[12] R. Seshadari, N.A. Hill, Chem. Mater. 13 (2001) 2892.
[13] C.J. Fennie, K.M. Rabe, Phys. Rev. B 72 (2005) 100103(R).
[14] B.B. Van Aken, T.T. Palstra, A. Filippetti, N.A. Spaldin, Nat. Mater. 3 (2004) 164.
[15] A. Malashevich, D. Vanderbilt, Eur. Phys. J. B 71 (2009) 345.
[16] P. Zubko, S. Gariglio, M. Gabay, P. Ghosez, J.-M. Triscone, Annu. Rev. Condens. Matter Phys. 2 (2011) 141.
[17] N.A. Hill, J. Phys. Chem. B 104 (2000) 6694.
[18] P. Baettig, N.A. Spaldin, Appl. Phys. Lett. 86 (2005) 012505.
[19] R. Nechache, C. Harnagea, A. Pignolet, F. Normandin, T. Veres, L.-P. Carignan, D. Ménard, Appl. Phys. Lett. 89 (2006) 102902.
[20] R. Nechache, C. Harnagea, L.-P. Carignan, O. Gautreau, L. Pintilie, M.P. Singh, D. Ménard, P. Fournier, M. Alexe, A. Pignolet, J. Appl. Phys. 95 (2009) 061621.
[21] P. Hohenberg, W. Kohn, Phys. Rev. 136 (1964) B864.
[22] W. Kohn, L. Sham, Phys. Rev. 140 (1965) A1133.
[23] R.M. Martin, Electronic Structure: Basic Theory and Practical Methods, Cambridge University Press, 2004.
[24] S. Baroni, P. Giannozzi, A. Testa, Phys. Rev. Lett. 58 (1987) 1861.
[25] X. Gonze, D.C. Allan, M.P. Teter, Phys. Rev. Lett. 68 (1992) 3603.
[26] X. Gonze, C. Lee, Phys. Rev. B 55 (1997) 10355.
[27] S. Baroni, S. de Gironcoli, A. Dal Corso, P. Giannozzi, Rev. Mod. Phys. 73 (2001) 515.
[28] X. Wu, D. Vanderbilt, D.R. Hamann, Phys. Rev. B 72 (2005) 035105.
[29] R.D. King-Smith, D. Vanderbilt, Phys. Rev. B 47 (1993) 1651.
[30] D. Vanderbilt, R. King-Smith, Phys. Rev. B 48 (1993) 4442.
[31] R. Resta, Ferroelectrics 136 (1992) 51.
[32] R. Resta, Rev. Mod. Phys. 66 (1994) 899.
[33] X. Gonze, P. Ghosez, R. Godby, Phys. Rev. Lett. 74 (1995) 4035.
[34] N. Sai, K.M. Rabe, D. Vanderbilt, Phys. Rev. B 66 (2002) 104108.
[35] I. Souza, J. Íñiguez, D. Vanderbilt, Phys. Rev. Lett. 89 (2002) 117602.
[36] M. Stengel, N.A. Spaldin, D. Vanderbilt, Nat. Phys. 5 (2009) 304.

[37] U. von Barth, L. Hedin, J. Phys. C 5 (1972) 1629.
[38] T. Thonhauser, D. Ceresoli, D. Vanderbilt, R. Resta, Phys. Rev. Lett. 95 (2005) 137205.
[39] D. Xiao, J. Shi, Q. Niu, Phys. Rev. Lett. 95 (2005) 137204.
[40] D. Ceresoli, U. Gerstmann, A.P. Seitsonen, F. Mauri, Phys. Rev. B 81 (2010) 060409.
[41] R. Resta, J. Phys. Condens. Matter 22 (2010) 123201.
[42] A. Malashevich, I. Souza, S. Coh, D. Vanderbilt, New J. Phys. 12 (2010) 053032.
[43] E. Bousquet, N.A. Spaldin, K.T. Delaney, Phys. Rev. Lett. 106 (2011) 107202.
[44] J. Iñiguez, Phys. Rev. Lett. 101 (2008) 117201.
[45] J.C. Wojdel, J. Iñiguez, Phys. Rev. Lett. 103 (2009) 267205.
[46] A. Malashevich, S. Coh, I. Souza, D. Vanderbilt, Phys. Rev. B 86 (2012) 094430.
[47] A. Scaramucci, E. Bousquet, M. Fechner, M. Mostovoy, N.A. Spaldin, Phys. Rev. Lett. 109 (2012) 197203.
[48] M. Ye, D. Vanderbilt, Phys. Rev. B 89 (2014) 064301.
[49] J.C. Wojdel, J. Iñiguez, Phys. Rev. Lett. 105 (2010) 037208.
[50] A.M. Essin, J.E. Moore, D. Vanderbilt, Phys. Rev. Lett. 102 (2009) 146805.
[51] A. Malashevich, I. Souza, S. Coh, D. Vanderbilt, New J. Phys. 12 (2010) 053032.
[52] A.M. Essin, A.M. Turner, J.E. Moore, D. Vanderbilt, Phys. Rev. B 81 (2010) 205104.
[53] M. Mostovoy, A. Scaramucci, N.A. Spaldin, K.T. Delaney, Phys. Rev. Lett. 105 (2010) 087202.
[54] S. Prosandeev, I.A. Kornev, L. Bellaiche, Phys. Rev. B 83 (2011) 020102.
[55] D. Rahmedov, D. Wang, J. Íñiguez, L. Bellaiche, Phys. Rev. Lett. 109 (2012) 037207.
[56] V.I. Anisimov, J. Zaanen, O.K. Andersen, Phys. Rev. B 44 (1991) 943.
[57] A.I. Liechtenstein, V.I. Anisimov, J. Zaanen, Phys. Rev. B 52 (1995) R5467.
[58] S.L. Dudarev, G.A. Botton, S.Y. Savrasov, C.J. Humphreys, A.P. Sutton, Phys. Rev. B 57 (1998) 1505.
[59] M. Cococcioni, S. de Gironcoli, Phys. Rev. B 71 (2005) 035105.
[60] I.A. Kornev, S. Lisenkov, R. Haumont, B. Dkhil, L. Bellaiche, Phys. Rev. Lett. 99 (2007) 227602.
[61] E. Bousquet, N.A. Spaldin, Phys. Rev. B 82 (2010) 220402.
[62] M. Goffinet, P. Hermet, D.I. Bilc, P. Ghosez, Phys. Rev. B 79 (2009) 014403.
[63] A. Stroppa, S. Picozzi, Phys. Chem. Chem. Phys. 12 (2010) 5405.
[64] J. Varignon, P. Ghosez, Phys. Rev. B 87 (2013) 140403(R).
[65] A. Prikockyte, D. Bilc, P. Hermet, C. Dubourdieu, P. Ghosez, Phys. Rev. B 84 (2011) 214301.
[66] J. Hong, A. Stroppa, J.J. Iïguez, S. Picozzi, D. Vanderbilt, Phys. Rev. B 85 (2012) 054417.
[67] C. Lee, W. Yang, R.G. Parr, Phys. Rev. B 37 (1988) 785.
[68] J. Heyd, G.E. Scuseria, M. Ernzerhof, J. Chem. Phys. 118 (2003) 8207.
[69] D.I. Bilc, R. Orlando, R. Shaltaf, G.-M. Rignanese, J. Íñiguez, P. Ghosez, Phys. Rev. B 77 (2008) 165107.
[70] A. Filippetti, N.A. Spaldin, Phys. Rev. B 67 (2003) 125109.
[71] A. Georges, G. Kotliar, W. Krauth, M.J. Rozenberg, Rev. Mod. Phys. 68 (1996) 13–125.
[72] G. Kotliar, S.Y. Savrasov, K. Haule, V.S. Oudovenko, O. Parcollet, C.A. Marianetti, Rev. Mod. Phys. 78 (2006) 865.
[73] A. Gellé, J. Varignon, M.-B. Lepetit, Europhys. Lett. 88 (2009) 37003.
[74] J. Varignon, S. Petit, A. Gellé, M.B. Lepetit, J. Phys. Condens. Matter 25 (2013) 496004.
[75] W. Zhong, D. Vanderbilt, K.M. Rabe, Phys. Rev. Lett. 73 (1994) 1861.
[76] W. Zhong, D. Vanderbilt, K.M. Rabe, Phys. Rev. B 52 (1995) 6301.
[77] S.P.I. Kornev, L. Bellaiche, Phys. Rev. B 83 (2011) 020102.
[78] S. Bhattacharjee, D. Rahmedov, D. Wang, J. Íñiguez, L. Bellaiche, Phys. Rev. Lett. 112 (2014) 147601.
[79] I.C. Infante, S. Lisenkov, B. Dupé, M. Bibes, S. Fusil, E. Jacquet, G. Geneste, S. Petit, A. Courtial, J. Juraszek, L. Bellaiche, A. Barthélémy, B. Dkhil, Phys. Rev. Lett. 105 (2010) 057601.
[80] S. Lisenkov, D. Rahmedov, L. Bellaiche, Phys. Rev. Lett. 103 (2009) 047204.
[81] J.H. Haeni, P. Irvin, W. Chang, R. Uecker, P. Reiche, Y.L. Li, S. Choudhury, W. Tian, M.E. Hawley, B. Craigo, A.K. Tagantsev, X.Q. Pan, S.K. Streiffer, L.Q. Chen, S.W. Kirchoefer, J. Levy, D.G. Schlom, Nature 430 (2004) 758.
[82] P. Ghosez, J.M. Triscone, Nat. Mater. 10 (2011) 269.
[83] S. Bhattacharjee, E. Bousquet, P. Ghosez, Phys. Rev. Lett. 102 (2009) 117602.
[84] T. Günter, E. Bousquet, A. David, P. Boullay, P. Ghosez, W. Prellier, M. Fiebig, Phys. Rev. B 85 (2012) 214120.
[85] E. Bousquet, N.A. Spaldin, Phys. Rev. Lett. 107 (2011) 197603.
[86] L. Bellaiche, Z. Gui, I.A. Kornev, J. Phys. Condens. Matter 24 (2012) 312201.
[87] T. Birol, N.A. Benedek, H. Das, A. Wysocki, A.T. Mulder, B.M. Abbett, E.H. Smith, S. Ghosh, C.J. Fennie, Curr. Opin. Solid State Mater. Sci. 16 (2012) 227.
[88] C.J. Fennie, Phys. Rev. Lett. 100 (2008) 167203.
[89] T. Varga, A. Kumar, E. Vlahos, S. Denev, M. Park, S. Hong, T. Sanehira, Y. Wang, C.J. Fennie, S.K. Streiffer, X. Ke, P. Schiffer, V. Gopalan, J.F. Mitchell, Phys. Rev. Lett. 103 (2009) 047601.
[90] H. Béa, B. Dupé, S. Fusil, R. Mattana, E. Jacquet, B. Warot-Fonrose, F. Wilhelm, A. Rogalev, S. Petit, V. Cros, A. Anane, F. Petroff, K. Bouzehouane, G. Geneste, B. Dkhil, S. Lisenkov, I. Ponomareva, L. Bellaiche, M. Bibes, A. Barthélémy, Phys. Rev. Lett. 102 (2009) 217603.
[91] O. Diéguez, O.E. González-Vázquez, J.C. Wojdeł, J. Íñiguez, Phys. Rev. B 83 (2011) 094105.
[92] Y. Yang, W. Ren, M. Stengel, X.H. Yan, L. Bellaiche, Phys. Rev. Lett. 109 (2012) 057602.
[93] Y. Yang, J. Íñiguez, A.-J. Mao, L. Bellaiche, Phys. Rev. Lett. 112 (2014) 057202.
[94] G. Song, W. Zhang, Sci. Rep. 4 (2014) 4564.
[95] E. Bousquet, N.A. Spaldin, P. Ghosez, Phys. Rev. Lett. 104 (2010) 037601.
[96] C. Escorihuela-Sayalero, O. Dièguez, J. Ìñiguez, Phys. Rev. Lett. 109 (2012) 247202.
[97] W. Baltensperger, J. Appl. Phys. 41 (1970) 1052.
[98] R.F. Sabiryanov, S.S. Jaswal, Phys. Rev. Lett. 83 (1999) 2062.
[99] C.J. Fennie, K.M. Rabe, Phys. Rev. Lett. 97 (2006) 267602.
[100] K.M. Rabe, P. Ghosez, Top. Appl. Phys. 105 (2007) 117.
[101] J.H. Lee, L. Fang, E. Vlahos, X. Ke, Y.W. Jung, L.F. Kourkoutis, J.-W. Kim, P.J. Ryan, T. Heeg, M. Roeckerath, V. Goian, M. Bernhagen, R. Uecker, P.C. Hammel, K.M. Rabe, S. Kamba, J. Schubert, J.W. Freeland, D.A.M.C.J. Fennieand, P. Schiffer, V. Gopalan, E. Johnston-Halperin, D.G. Schlom, Nature 466 (2010) 954.
[102] O. Chmaissem, B. Dabrowski, S. Kolesnik, J. Mais, D.E. Brown, R. Kruk, P. Prior, B. Pyles, J.D. Jorgensen, Phys. Rev. B 64 (2001) 134412.
[103] J.H. Lee, K.M. Rabe, Phys. Rev. Lett. 104 (2010) 207204.
[104] R. Schleck, Y. Nahas, R.S.P.M. Lobo, J. Varignon, M.B. Lepetit, C.S. Nelson, R.L. Moreira, Phys. Rev. B 82 (2010) 054412.

[105] S. Artyukhin, K.T. Delaney, N.A. Spaldin, M. Mostovoy, Nat. Mater. 13 (2014) 42.
[106] A. Levanyuk, D.G. Sannikov, Phys. Usp. 17 (1974) 199.
[107] N. Sai, C.J. Fennie, A.A. Demkov, Phys. Rev. Lett. 102 (2009) 107601.
[108] M. Stengel, C.J. Fennie, P. Ghosez, Phys. Rev. B 86 (2012) 094112.
[109] Q. Zhou, K.M. Rabe, arXiv:1306.1839.
[110] J.M. Perez-Mato, M. Aroyo, A. García, P. Blaha, K. Schwarz, J. Schweifer, K. Parlinski, Phys. Rev. B 70 (2004) 214111.
[111] E. Bousquet, M. Dawber, N. Stucki, C. Lechtensteiger, P. Hermet, S. Gariglio, J.M. Gariglio, P. Ghosez, Nature 452 (2008) 732.
[112] N.A. Benedek, C.J. Fennie, Phys. Rev. Lett. 106 (2011) 107204.
[113] P. Aguado-Puente, P. García-Fernàndez, J. Junquera, Phys. Rev. Lett. 107 (2011) 217601.
[114] T. Fukushima, A. Stroppa, S. Picozzi, J.M. Perez-Mato, Phys. Chem. Chem. Phys. 13 (2011) 12186.
[115] J.M. Rondinelli, C.J. Fennie, Adv. Mater. 24 (2010) 1964.
[116] A. Stroppa, P. Barone, P. Jain, J.M. Perez-Mato, S. Picozzi, Adv. Mater. 25 (2013) 2284.
[117] A.T. Mulder, N.A. Benedek, J.M. Rondinelli, C.J. Fennie, Adv. Funct. Mater. 23 (2013) 4810.
[118] J. Young, J.M. Rondinelli, Phys. Rev. B 89 (2014) 174110.
[119] H.J. Zhao, W. Ren, Y. Yang, J. Íñiguez, X.M. Chen, L. Bellaiche, Nat. Commun. 5 (2014) 4021.
[120] Z. Zanolli, J.C. Wojdel, J. Iñiguez, P. Ghosez, Phys. Rev. B 88 (2013) 060102(R).
[121] I. Etxebarria, J. Perez-Mato, P. Boullay, Ferroelectrics 401 (2010) 17.
[122] K. Yamauchi, P. Barone, J. Phys. Condens. Matter 26 (2014) 103201.
[123] A. Malashevich, D. Vanderbilt, Phys. Rev. Lett. 101 (2008) 037209.
[124] A.M. Noz, M.T. Casáis, J.A. Alonso, M.J. Martínez-Lope, J.L. Matrínez, M.T. Fernández-Diaz, Inorg. Chem. 40 (2001) 1020.
[125] J.S. Zhou, J.B. Goodenough, Phys. Rev. Lett. 96 (2006) 247202.
[126] J.-S. Zhou, J.B. Goodenough, B. Dabrowski, Phys. Rev. Lett. 95 (2005) 127204.
[127] S. Picozzi, K. Yamauchi, B. Sanyal, I.A. Sergienko, E. Dagotto, Phys. Rev. Lett. 99 (2007) 227201.
[128] K. Yamauchi, F. Freimuth, S. Blugel, S. Picozzi, Phys. Rev. B 78 (2008) 014403.
[129] G. Giovannetti, J. van den Brink, Phys. Rev. Lett. 100 (2008) 22703.
[130] T.-R. Chang, H.-T. Jeng, C.-Y. Ren, C.-S. Hsue, Phys. Rev. B 84 (2011) 024421.
[131] S. Partzsch, S.B. Wilkins, J.P. Hill, E. Schierle, E. Weschke, D. Souptel, B. Büchner, J. Geck, Phys. Rev. Lett. 107 (2011) 057201.
[132] D.V. Efremov, J.V. den Brinck, D. Khomskii, Nat. Mater. 3 (2004) 853.
[133] C. Ederer, N.A. Spaldin, Nat. Mater. 3 (2004) 851.
[134] A.M. Kadomtseva, Y.F. Popov, G.P. Vorob'ev, K.I. Kamilov, V.Y. Ivanov, A.A. Mukhin, A.M. Balbashov, J. Exp. Theor. Phys. 106 (2008) 130.
[135] G. Giovannetti, S. Kumar, J.V. den Brinck, S. Picozzi, Phys. Rev. Lett. 103 (2009) 037601.
[136] K. Kato, S. Iida, K. Yanai, K. Mizushima, J. Magn. Magn. Mater. 31 (1983) 783.
[137] K. Yamauchi, T. Fukushima, S. Picozzi, Phys. Rev. B 79 (2009) 212404.
[138] M. Alexe, M. Ziese, D. Hesse, P. Esquinazi, K. Yamauchi, T. Fukushima, S. Picozzi, U. Gösele, Adv. Mater. 21 (2009) 4452.
[139] N. Ikeda, H. Ohsumi, K. Ohwada, K. Ishii, T. Inami, K. Kakurai, Y. Murakami, S. Yoshii, S. Mori, Y. Horibe, H. Kitô, Nature 436 (2005) 1136.
[140] M. Angst, R.P. Hermann, A.D. Christianson, M.D. Lumsden, C. Lee, M.-H. Whangbo, J.-W. Kim, P.J. Ryan, S.E. Nagler, W. Tian, R. Jin, B.C. Sales, D. Mandrus, Phys. Rev. Lett. 101 (2008) 227601.
[141] V. Pardo, S. Blanco-Canosa, F. Rivadulla, D.I. Khomskii, D. Baldomir, H. Wu, J. Rivas, Phys. Rev. Lett. 101 (2008) 256403.
[142] G. Giovannetti, A. Stroppa, S. Picozzi, D. Baldomir, V. Pardo, S. Blanco-Canosa, F. Rivadulla, S. Jodlauk, D. Niermann, J. Rohrkamp, T. Lorenz, S. Streltsov, D.I. Khomskii, J. Hemberger, Phys. Rev. B 83 (2011) 060402(R).
[143] K. Yamauchi, T. Oguchi, S. Picozzi, J. Phys. Soc. Jpn. 83 (2014) 094712.
[144] K. Yamauchi, S. Picozzi, Phys. Rev. Lett. 105 (2010) 107202.
[145] N. Ogawa, Y. Ogimoto, Y. Ida, Y. Nomura, R. Arita, K. Miyano, Phys. Rev. Lett. 108 (2012) 157603.
[146] K. Gupta, P. Mahadevan, P. Mavropoulos, M. Ležaic, Phys. Rev. Lett. 111 (2013) 077601.
[147] H. Zheng, J. Wang, S.E. Lofland, Z. Ma, L. Mohaddes-Ardabili, T. Zhao, L. Salamanca-Riba, S.R. Shinde, S.B. Ogale, F. Bai, D. Viehland, Y. Jia, D.G. Schlom, M. Wuttig, A. Roytburd, R. Ramesh, Science 303 (2004) 661.
[148] H. Yamada, Y. Ogawa, Y. Ishii, H. Sato, M. Kawasaki, H. Akoh, Y. Tokura, Science 305 (2004) 646.
[149] Y. Wang, J. Hu, Y. Lin, C.W. Nan, NPG Asia Mater. 2 (2010) 61.
[150] J.P. Velev, S.S. Jaswal, E.Y. Tysmbal, Philos. Trans. R. Soc. Lond. A 369 (2011) 3069.
[151] C.A.F. Vaz, J. Phys. Condens. Matter 24 (2012) 333201.
[152] C.A.F. Vaz, J. Hoffman, C.H. Ahn, R. Ramesh, Adv. Mater. 22 (2010) 2900.
[153] M. Stengel, N.A. Spaldin, Phys. Rev. B 75 (2007) 205121.
[154] M. Stengel, N. Spaldin, Nature 443 (2006) 679.
[155] M. Stengel, P. Aguado-Puente, N.A. Spaldin, J. Junquera, Phys. Rev. B 83 (2011) 235112.
[156] D.D. Sante, K. Yamauchi, S. Picozzi, J. Phys. Condens. Matter 25 (2013) 066001.
[157] H. Chen, S. Ismael-Beigi, Phys. Rev. B 86 (2012) 024433.
[158] R. Ramesh, Nat. Nanotechnol. 3 (2008) 7.
[159] J.M. Rondinelli, M. Stengel, N.A. Spaldin, Nat. Nanotechnol. 3 (2008) 46.
[160] M.K. Niranjan, J.D. Burton, J.P. Velev, S.S. Jaswal, E.Y. Tsymbal, Appl. Phys. Lett. 95 (2009) 052501.
[161] C.-G. Duan, C.W. Nan, S.S. Jaswal, E. Tsymbal, Phys. Rev. B 79 (2009) 140403.
[162] C.-G. Duan, J.P. Velev, R.F. Sabirianov, Z. Zhu, J. Chu, S.S. Jaswal, E.Y. Tsymbal, Phys. Rev. Lett. 101 (2008) 137201.
[163] C.-G. Duan, S.S. Jaswal, E.Y. Tsymbal, Phys. Rev. Lett. 97 (2006) 047201.
[164] M. Fechner, I.V. Maznichenko, S. Ostanin, A. Ernst, J. Henk, P. Bruno, I. Mertig, Phys. Rev. B 78 (2008) 212406.
[165] J. Lee, N. Sai, T. Cai, Q. Niu, A. Demkov, Phys. Rev. B 81 (2010) 144425.
[166] K. Yamauchi, B. Sanyal, S. Picozzi, Appl. Phys. Lett. 91 (2007) 062506.
[167] M.K. Niranjan, J.P. Velev, C.G. Duan, S.S. Jaswal, E.Y. Tsymbal, Phys. Rev. B 78 (2008) 104405.
[168] J.D. Burton, E.Y. Tsymbal, Phys. Rev. B 80 (2009) 174406.
[169] N.C. Bristowe, M. Stengel, P.B. Littlewood, J.M. Pruneda, E. Artacho, Phys. Rev. B 85 (2012) 024106.
[170] C.-G. Duan, J. Valev, R.F.S.W.N. Mei, S.S. Jaswal, E.Y. Tsymbal, Appl. Phys. Lett. 92 (2008) 122905.
[171] K. Nakamura, R. Shimabukuro, Y. Fujiwara, T. Akiyama, T. Ito, A. Freeman, Phys. Rev. Lett. 102 (2009) 187201.
[172] M. Tsujikawa, T. Oda, Phys. Rev. Lett. 102 (2009) 247203.
[173] H. Zhang, M. Ritcher, K. Koepernik, I. Opahle, F. Tasnadi, H. Eschrig, New J. Phys. 11 (2009) 043007.
[174] M.K. Niranjan, C.-G. Duan, S.S. Jaswal, E.Y. Tsymbal, Appl. Phys. Lett. 96 (2010) 222504.
[175] P.V. Lukashev, J.D. Burton, S.S. Jaswal, E.Y. Tsymbal, J. Phys. Condens. Matter 24 (2012) 226003.

[176] M. Fechner, P. Zahn, S. Ostanin, M. Bibes, I. Mertig, Phys. Rev. Lett. 108 (2012) 197206.
[177] A. Sadoc, B. Mercey, C. Simon, D. Grebille, W. Prellier, M.-B. Lepetit, Phys. Rev. Lett. 104 (2010) 046804.
[178] H. Chen, Q. Qiao, M.S.J. Marshall, A.B. Georgescu, A. Gulec, P.J. Phillips, R.F. Klie, F.J. Walker, C.H. Ahn, S. Ismail-Beigi, Nano Lett. 14 (2014) 4965.
[179] J. Seidel, L.W. Martin, Q. He, Q. Zhan, Y.-H. Chu, A. Rother, M.E. Hawkridge, P. Maksymovych, P. Yu, M. Gajek, N. Balke, S.V. Kalinin, S. Gemming, F. Wang, G. Catalan, J.F. Scott, N.A. Spaldin, J. Orenstein, R. Ramesh, Nat. Mater. 8 (2009) 229.
[180] S. Farokhipoor, C. Magén, S. Venkatesan, J. Ìñiguez, C.J.M. Daumont, D. Rubi, E. Snoeck, M. Mostovoy, C. de Graaf, A. Müller, M. Döblinger, C. Scheu, B. Noheda, Nat. Mater. 515 (2014) 379.
[181] Ph. Ghosez, J.M. Triscone, Nat. Mater. 515 (2014) 348.
[182] H. Das, A.L. Wysocki, Y. Geng, W. Wu, C.J. Fennie, Nat. Commun. 5 (2014) 1.
[183] Y. Geng, H. Das, A.L. Wysocki, X. Wang, S.-W. Cheong, M. Mostovoy, C.J. Fennie, W. Wu, Nat. Mater. 13 (2014) 163.
[184] W. Setyawan, S. Curtarolo, Comput. Mater. Sci. 49 (2010) 299.
[185] G. Hautier, A. Jain, S.P. Ong, J. Mater. Sci. 47 (2012) 7317.
[186] A. Jain, S.P. Ong, G. Hautier, W. Chen, W.D. Richards, S. Dacek, S. Cholia, D. Gunter, D. Skinner, G. Ceder, K.A. Persson, APL Mater. 1 (2013) 011002.
[187] J.W. Bennett, K.F. Garrity, K.M. Rabe, D. Vanderbilt, Phys. Rev. Lett. 109 (2012) 167602.